

Processing and Characterization of High Q_m Ferroelectric Ceramics

C. Galassi,^{a*} E. Roncari,^a C. Capiani^a and F. Craciun^b

^aCNR Istituto di Ricerche Tecnologiche per la Ceramica, via Granarolo 64, I-48018 Faenza, Italy

^bCNR Istituto di Acustica “O.M. Corbino”, Area di Ricerca Tor Vergata, via del Fosso del Cavaliere 100, I-00133 Roma, Italy

Abstract

Use of ferroelectric ceramics in applications like piezoelectric transformers was made possible by the development of new materials with high electro-mechanical coupling coefficients and high mechanical quality factor. “Hard” ferroelectric ceramics of complex composition based on lead zirconate titanate with Nb, Mg, Mn and Li additives have been prepared. The perovskitic phase was produced by solid phase reaction of the oxides. The crucial role played by the intermediate mixing and grinding procedures in the assessment of the final properties of the material was investigated. Densification up to approximately the theoretical density value was achieved. The polarization was obtained by subjecting the samples at 30 kV cm^{-1} poling electric field, in a silicon oil bath heated at 120°C . Their structural and morphological properties were checked by X-ray diffraction analysis and scanning electron microscopy. Ferroelectric and piezoelectric properties were determined in agreement with IEEE measurement standards. The optimized samples presented very high quality and electromechanical coupling factors, together with small dielectric loss. © 1999 Elsevier Science Limited. All rights reserved

Keywords: powders-solid state reaction, piezoelectric properties, PZT.

1 Introduction

In order to match the specific requirements for the wide range of applications for materials in the $\text{Pb}(\text{ZrTi})\text{O}_3$ (PZT) system either compositional modifications and novel or improved processing routes have been intensively investigated. For the

use as actuators or transformers it is desirable to combine high mechanical quality factor (Q_m) with high piezoelectric constant (d) and high planar coupling factor (k_p). The role of several dopants either donor or acceptor type added separately or in combination¹ has been clarified as well as the properties of ternary or more complex solid solutions^{2–4} resulted much improved. All the compositions are close to the morphotropic phase boundary (MPB), and are partially substituted by $\text{Pb}(\text{Mg}_{1/3}\text{Nb}_{2/3})$, $\text{Pb}(\text{Y}_{2/3}\text{W}_{1/3})$, $\text{Pb}(\text{Ni}_{1/3}\text{Nb}_{2/3})$ solid solution systems. Iso-valent modifiers like MnO_2 , La_2O_3 , Fe_2O_3 , SiO_2 etc., are added that act as “hardener” or “softener” of the elasto-piezoelectric properties and control sintering kinetics and grain growth. It is well known that the combination of donor doping, e.g. Nb^{5+} (which increases permittivity, elastic compliance and coupling coefficients) with acceptor doping like Mg^{2+} , Li^+ , and specifically MnO_2 making ions Mn^{3+} and Mn^{2+} in the solid solution (which increases mechanical Q and coercivity) is required to ensure acceptable properties of the material. Apart from the role played as aliovalent substituents in determining the point defects in the lattice structure the added ions contribute to the formation of the microstructure, noticeably grain size which in turn influences domain-wall motion and so final properties.⁵ Perovskitic phase synthesis by reaction of the starting oxides in the solid phase followed by cold consolidation and densification still receives a great deal of interest because correlation of the final properties with the modifications introduced during the different processing steps has not yet unambiguously clarified.

The objective of this paper is to study the influence of processing modification (milling introduced at different steps of the powder treatments) on the microstructure and dielectric and piezoelectric properties of a multicomponent complex PZT system that exhibits good properties for piezoelectric transformer.^{6,7}

*To whom correspondence should be addressed. Fax: +39-0546-46381; e-mail: carmen@irtecl.irtec.bo.cnr.it

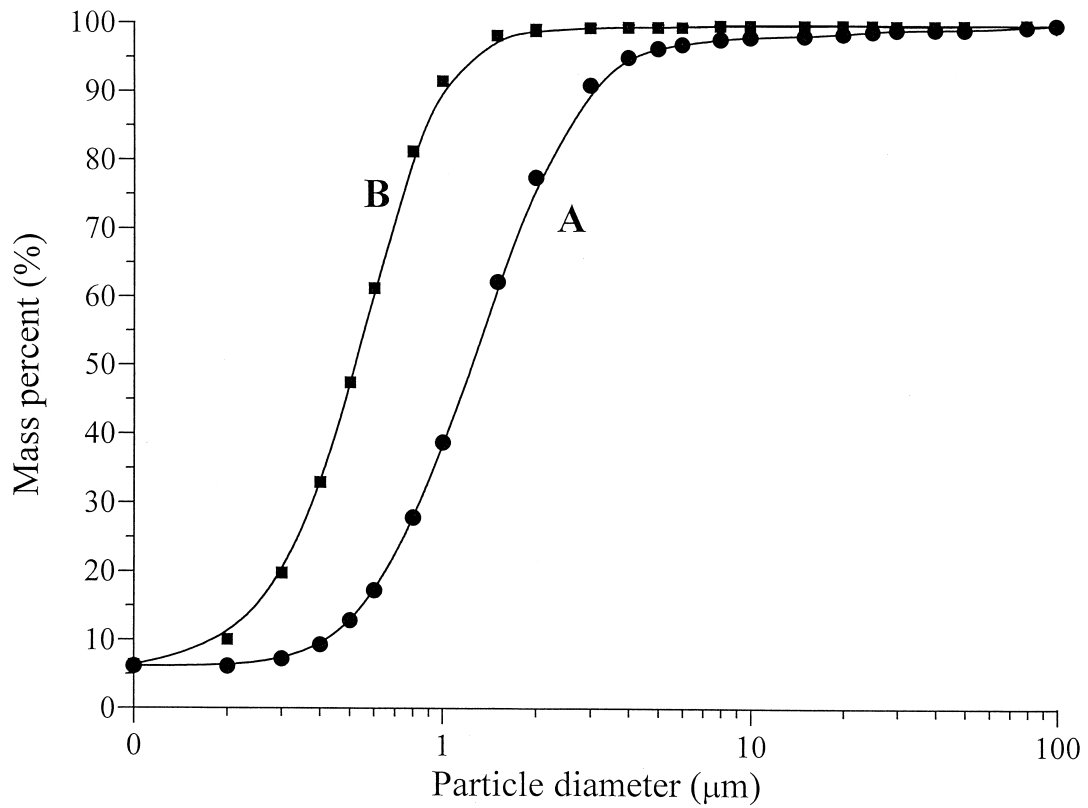


Fig. 1. Particle size distribution of (A) powder crushed and (B) ball milled 100 h.

Table 1. Processing parameters, density and shrinkage of the PZT samples

Sample	Grinding procedure	Green density		Sintered density		Shrinkage (%)	Weight loss (%)
		($g\ cm^{-3}$)	(%)	($g\ cm^{-3}$)	(%)		
A	Agate mortar after calcination	5.07	64.2	7.88	99.7	13.1	0.5
B	Wet milling after calcination for 100 h	4.77	60.4	7.90	100.0	15.3	0.4
C	Sample A with MnO_2 pre-ground	4.53	57.4	7.86	99.5	14.0	0.7

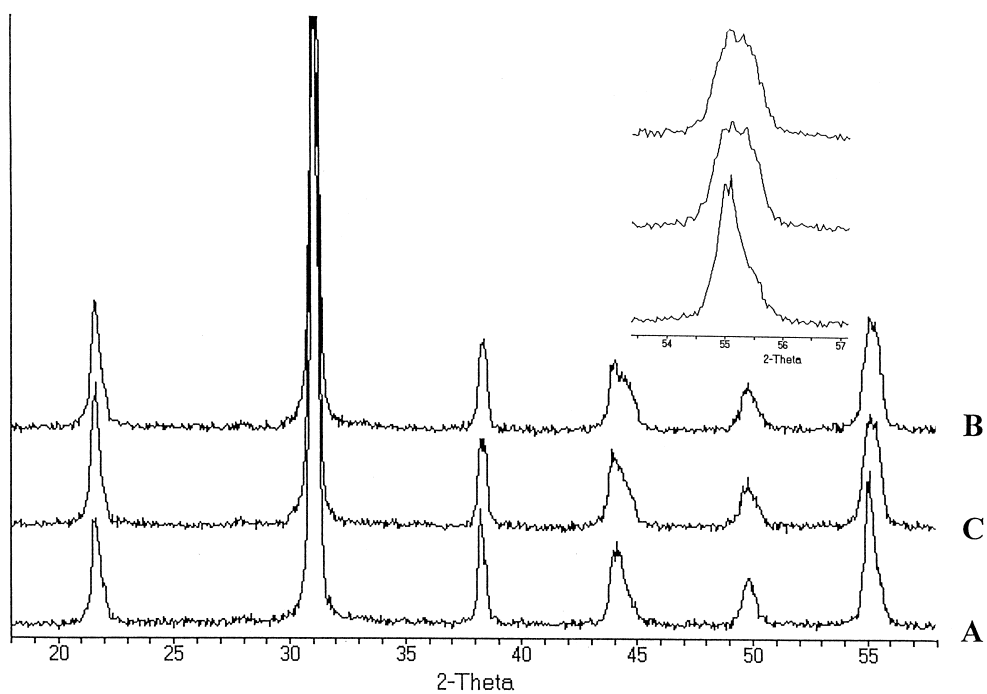


Fig. 2. XRD patterns of the sintered samples with the enlargement of the 200 reflection.

2 Experimental Procedure

Starting from reagent grade PbO (Aldrich), ZrO₂ (MEL SC101), TiO₂ (Degussa P25), Nb₂O₅ (Fluka), MgO (Carlo Erba), Li₂CO₃ (Merck) and MnO₂ (Fluka) the PZT material of the composition $[\text{Pb}(\text{Li}_{0.25}\text{Nb}_{0.75})]_{0.06}[\text{Pb}(\text{Mg}_{0.33}\text{Nb}_{0.67})]_{0.06}[\text{Pb}(\text{Zr}_{0.50}\text{Ti}_{0.50})]_{0.88}\text{O}_3$ added with 0.7wt% MnO₂ was prepared. The raw materials were mixed in water for 72 h, freeze dried, sieved to 250 μm and calcined at 850°C for 4 h. The calcined powder either dry crushed in an agate mortar (sample A) or wet milled in ethanol for 100 h (sample B), was then dried, sieved, granulated and cold isostatically pressed at 150 MPa into discs of 30 mm diameter or pellets of square or rectangular shape as required for the standard electrical characterization. Being the as received MnO₂ a very coarse raw material (6wt% smaller than 75 μm) another sample was prepared by adding the MnO₂ powder, separately pre ground in agate mortar, to the batch of the oxides following the same process of the sample A (sample C). After sintering at 1200°C for 2 h in lead atmosphere maintained by a PbZrO₃ source in a closed Al₂O₃ crucible, the samples were ground to remove surface layers, screen printed with silver electrodes, fired at 700°C and finally poled into silicon oil at 120°C, under a d.c. field of 3 kV mm⁻¹ for 40 min.

Density of the sintered samples was measured by the Archimedes method while the green density was geometrically measured; crystallographic structure was identified by X-ray diffraction technique (XRD), particle size distribution was measured by X-ray sedimentation technique and microstructure was analyzed with a scanning electron microscope (SEM).

Samples with shapes and dimensions recommended by the IEEE standards were prepared for piezoelectric characterization. On each sample the electrical impedance was measured as a function of frequency by using an HP4194A impedance bridge. From the values of resonance and antiresonance frequencies of certain selected modes, together with the minimum impedance, capacitance, density and geometrical dimensions, the piezoelectric, dielectric and elastic coefficients, as well as the electro-mechanical coupling factors and the mechanical quality factor Q_m have been determined.

3 Results and Discussion

3.1 Microstructure

The as calcined powders present very similar diffraction patterns of a rhombohedral perovskitic phase with a slight enlargement of the 200 reflection

that is evidence of the coexistence of tetragonal phase. The particle size distribution of the powder A, crushed only in agate mortar and the powder B, ball milled after calcination is reported in Fig. 1. Ninety mass% of the powder B is in the sub-micrometer size range (mean diameter is 0.55 μm) while the average diameter of powder A is 1.22 μm . It reflects on the cold packing behavior which gives higher green density for the coarser powder A as reported in Table 1; both reach almost full density with a very low weight loss. The XRD patterns of the sintered samples are shown in Fig. 2; in all the

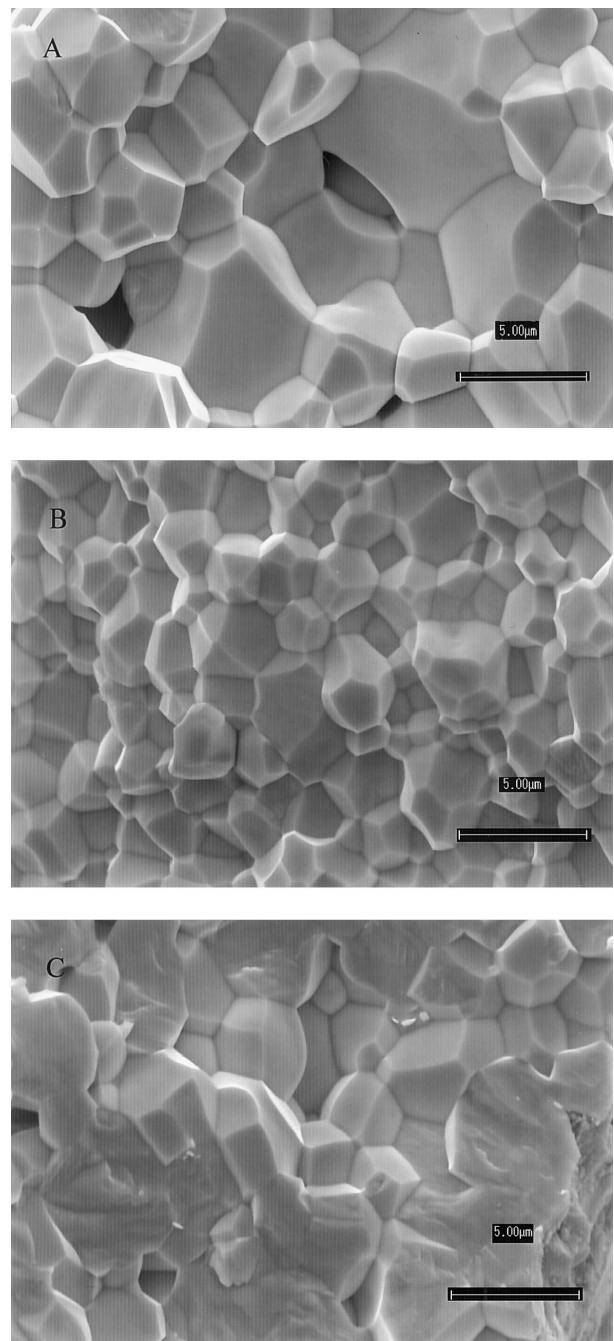


Fig. 3. SEM micrographs of the fracture of the sintered samples starting from (a) crushed powder, (b) ball milled powder and (c) using MnO₂ pre-ground in sample A.

Table 2. Piezoelectric and dielectric properties

Sample	ρ (10^3 kg m^{-3})	σ_p	k_p	k_{31}	d_{31} ($10^{-12} \text{ m V}^{-1}$)	g_{31} ($10^{-3} \text{ V m N}^{-1}$)	S_{11}^E ($10^{-12} \text{ m}^2 \text{ N}^{-1}$)	Q_m
A	7.88	0.40	0.32	-0.18	-50.0	-8.20	13.0	380
B	7.90	0.31	0.54	-0.32	-64.7	-16.34	10.64	2132
C	7.86	0.30	0.54	-0.34	-69.0	-16.28	10.95	994

samples the perovskitic phase is nearly rhombohedral (sample A) with an increasing amount of tetragonal phase (samples C and B). Strong differences in the microstructure are evidenced by the SEM pictures shown in Fig. 3: it is evidenced that sample A is rather homogeneous, the mean grain size is $2.8 \mu\text{m}$ and the fracture is intergranular, sample B is very homogeneous with mean grain size $1.9 \mu\text{m}$ and very intergranular fracture, sample C is less homogeneous, the fracture is essentially transgranular and the mean grain size is estimated around $2.5 \mu\text{m}$. The difference in microstructure between samples A and B can be explained taking into account the different particle size of the starting powders that induce higher grain growth and lower densification rate when they are coarser (sample A), a conventional solid state sintering mechanism can be supposed; in case of sample C the intragranular nature of the fracture following a more pronounced grain growth let us make the hypothesis that a liquid phase promoted densification takes place.

3.2 Electrical measurements

The comparison of dielectric and piezoelectric properties of the three samples is reported in Table 2. They all behave as “hard” piezoelectrics but sample A shows a very low coupling factor in comparison to B and C and the mechanical quality factor Q_m strongly increases from A to C to B which exhibits the best performance and is suitable for practical application as transformer. The full set of properties of sample B is reported in Table 3.

The microstructural characterization here carried out does not allow to support with experimental

evidence the full explanation of the differences in the performance but some comments can be drawn: it has been evidenced that the sintering of those complex compositions is supported by the formation of a transient liquid phase that in some cases does not disappear even in the final stage of sintering. In the present composition some of the aliovalent substituents can either enter the solid solution or be involved in the PbO containing liquid phase: the coarser is the starting powder, the fraction of substituents involved in the solid solution can be supposed lower so they participate in the formation of the transient liquid phase that promotes grain growth and then disappears in the final stage of sintering (sample A); this is not the case for sample B where they fully exert their role of acceptor dopants (Mg^{2+} , $\text{Mn}^{2/3/4+}$, Li^+), donor dopants (Nb^{5+}) or grain growth inhibitors. In the case of sample C the finer granulometry of the raw MnO_2 could allow a competition among the acceptor doping ions so that it enters the solid solution and improves substantially the Q_m factor while the other liquid phase promoting components give rise to a less viscous liquid phase that does not disappear in the final microstructure and enhances grain growth more than in case of sample A; the consequence is intermediate final properties.

4 Conclusions

The milling steps introduced during processing control the microstructure development and the dielectric and piezoelectric properties of the PZT samples. The best results were obtained by wet milling the calcined powder in ethanol for 100 h. An optimized material with Q_m as high as 2132 and K_p 0.54 was developed allowing suitable applications as transformer. The granulometry of the MnO_2 powder added to oxide mixture plays an important role to determine both microstructural and piezoelectric properties.

Acknowledgements

The authors gratefully acknowledge Anna Costa for SEM analysis and Alida Bellosi for helpful discussion on the sintering mechanism.

Table 3. Piezoelectric and dielectric properties of the optimized B composition

ρ (10^3 kg m^{-3})	7.9	Q_m	2132
k_{33}	0.67	C_{11}^E (10^{10} N m^{-2})	14.8
k_{31}	-0.31	C_{33}^E (10^{10} N m^{-2})	13.5
k_{15}	0.72	C_{44}^E (10^{10} N m^{-2})	3.3
k_p	0.54	C_{12}^E (10^{10} N m^{-2})	7.6
d_{33} ($10^{-12} \text{ m V}^{-1}$)	148.7	C_{13}^E (10^{10} N m^{-2})	-7.7
d_{31} ($10^{-12} \text{ m V}^{-1}$)	-64.7	S_{11}^E ($10^{-12} \text{ m}^2 \text{ N}^{-1}$)	10.6
d_{15} ($10^{-12} \text{ m V}^{-1}$)	392.0	S_{33}^E ($10^{-12} \text{ m}^2 \text{ N}^{-1}$)	12.3
g_{33} ($10^{-3} \text{ V m N}^{-1}$)	37.6	S_{44}^E ($10^{-12} \text{ m}^2 \text{ N}^{-1}$)	30.0
g_{31} ($10^{-3} \text{ V m N}^{-1}$)	-16.3	S_{12}^E ($10^{-12} \text{ m}^2 \text{ N}^{-1}$)	-3.0
g_{15} ($10^{-3} \text{ V m N}^{-1}$)	39.3	S_{13}^E ($10^{-12} \text{ m}^2 \text{ N}^{-1}$)	4.2
$\varepsilon_{33}^T = K_3^T$	447.2	σ_p	0.31
$\varepsilon_{11}^T = K_1^T$	1129	V_{tr} (m s^{-1})	3449

References

1. Park, J. H., Kim, B. K., Song, K. H. and Park, S. Ja., Piezoelectric properties of Nb_2O_5 doped and MnO_2 - Nb_2O_5 co-doped $\text{Pb}(\text{Zr}_{0.53}\text{Ti}_{0.47})\text{O}_3$. *J. Mat. Sc. Materials in Electronics*, 1995, **6**, 97–101.
2. Dong, D., Murakami, K., Kaneko, S. and Xiong, M., Piezoelectric properties of PZT ceramics sintered at low temperatures with complex-oxide additives. *J. Ceram. Soc. Jap Int. Ed.*, 1993, **101**, 1061–1065.
3. Wu, L., Liang, C. K. and Shieu, C. F., Piezoelectric properties of (Pb, Sr) (Zr, Ti, Mn, Zn, Nb) O_3 piezoelectric ceramics. *J. Mat. Sci.*, 1991, **26**, 4439–4444.
4. Yoon, S. J., Yoo, S. J., Moon, J. H., Jung, H. J. and Kim, H. J., Effects of La_2O_3 and MnO_2 on the piezoelectric properties of $0.02\text{Pb}(\text{Y}_{2/3}\text{W}_{1/3})\text{O}_3$ - $0.98\text{Pb}(\text{Zr}_{0.52}\text{Ti}_{0.48})\text{O}_3$. *J. Mat. Res.*, 1996, **11**(2), 348–352.
5. Randall, C. A., Kim, N., Kucera, J. P., Cao, W. and Shrout, T. R., Intrinsic and extrinsic size effects in fine-grained morphotropic lead zirconate titanate ceramics. *J. Am. Ceram. Soc.*, 1998, **81**(3), 677–688.
6. Bao, Y., Chen, A., Han, J. and Zhi, Y., A study of piezoelectric ceramics of $\text{Pb}(\text{Li}_{1/4}\text{Nb}_{3/4})\text{O}_3$ - $\text{Pb}(\text{Mg}_{1/3}\text{Nb}_{2/3})\text{O}_3$ - $\text{Pb}(\text{ZrTi})\text{O}_3$ system for transformer. In *Proceeding of the Electroceramics V*, Vol. 1, ed. J. L. Baptista, J. A. Labrincha and P. M. Vilarinho. University of Aveiro, 1996, pp. 237–240.
7. Cellucci, G., Pirani, S., Galassi, C., Capiani, C., Watts, B. E., Melioli, E. and Leccabue, F., The fabrication and testing of a piezoelectric transformer. *Ferroelectrics*, in press.